available at www.sciencedirect.com

ScienceDirect

journal homepage: www.ejconline.com

Patched haploinsufficient mouse rhabdomyosarcoma overexpress secreted phosphoprotein 1 and matrix metalloproteinases

Massimiliano De Bortoli[a,*], *Robert C. Castellino*[a], *Darlene G. Skapura*[a], *Jianhe J. Shen*[a], *Jack M. Su*[a], *Heidi V. Russell*[a], *M. John Hicks*[b], *Tsz-Kwong Man*[a], *John Y.H. Kim*[a]

[a]*Texas Children's Cancer Center, Department of Pediatrics, Baylor College of Medicine, 6621 Fannin Street, MC 3-3320 Houston, TX 77030, USA*

[b]*Texas Children's Hospital, Department of Pathology, Baylor College of Medicine, 6621 Fannin Street, MC 3-3320 Houston, TX 77030, USA*

ARTICLE INFO

Article history:
Received 5 December 2006
Received in revised form 14 February 2007
Accepted 14 February 2007

Keywords:
Rhabdomyosarcoma
Mouse model, *patched*
SPP1
NF-κB
Matrix metalloproteinase

ABSTRACT

Rhabdomyosarcoma is the most common soft tissue sarcoma of childhood. Improving the management of rhabdomyosarcoma requires a better understanding of growth regulation. *Patched* haploinsufficient (*Ptch+/–*) mice spontaneously develop soft tissue sarcomas that resemble human rhabdomyosarcomas. Using microarray profiling and quantitative real-time reverse transcriptase polymerase chain reaction, we identified candidate genes differentially expressed in *Ptch+/–* mouse rhabdomyosarcoma relative to mature muscle. Overexpressed genes include *Secreted Phosphoprotein 1* (*Spp1*, *Osteopontin*), and *Matrix Metalloproteinases-2* and -14 (*Mmp2* and *Mmp14*). *Spp1* is an integrin-binding phosphoglycoprotein upregulated in carcinomas, and Mmps regulate tumour invasion. Immunochemical analyses of murine and human rhabdomyosarcoma specimens confirmed increased expression of Spp1, Mmp2, Mmp14, nuclear factor-kappa B (NF-κB) p65 and its phosphorylated active isoform. Neutralising Spp1 antibody decreased *Mmp14* RNA in murine rhabdomyosarcoma cultures, indicating a positive regulatory role for extracellular Spp1. Plasma from rhabdomyosarcoma patients display elevated levels of SPP1. These results implicate Spp1, NF-κB, and Mmp activation as a putative signalling pathway involved in rhabdomyosarcoma growth.

1. Introduction

Rhabdomyosarcoma (RMS) is the most common soft tissue sarcoma of childhood and can arise in diverse anatomic locations.[1,2] Combined modality treatment with surgical resection, systemic chemotherapy and local radiation therapy has increased the overall survival of patients with localised RMS from only 25% in 1970 to 75% currently.[1,2] However, the prognosis remains grim for children with tumours that are metastatic, unresectable, large, or locally invasive.[1] High-stage and metastatic RMS continues to present challenges because of aggressive growth and treatment resistance, which disproportionately contribute to morbidity and mortality.[1,2] Further improving the management of RMS requires a better understanding of the mechanisms regulating tumour growth, invasion, and metastasis. Although the biological determi-

* *Corresponding author:* Tel.: +1 832 824 4395; fax: +1 832 825 4038.
E-mail address: jyhkim@kidstumor.org (J.Y.H. Kim).
0959-8049/$ - see front matter
doi:10.1016/j.ejca.2007.02.008

nants of clinical behaviour are being actively sought in the genetic lesions associated with RMS, the precise mechanisms involved in local tissue invasion and metastasis that constitute tumour progression remain elusive and ripe for gene discovery approaches.[1,2]

Because primary human RMS cells are difficult to manipulate and the derived cell lines are limited and artifactual, mouse models have emerged as essential experimental systems for basic studies and preclinical testing.[1,3] Increased risk of RMS is associated with mutation of *TP53* and PATCHED (*PTCH*) in patients with Li-Fraumeni and Gorlin syndromes, respectively.[4,5] The latter, also known as nevoid basal cell carcinoma syndrome (NBCCS), is associated with germline mutations of *PTCH*, which was targeted to generate a murine model.[6] *Patched* (Ptch) encodes the transmembrane receptor for the morphogen Sonic hedgehog (Shh), which is a key activator of myogenic progenitor differentiation.[7] Ptch negatively regulates downstream signalling via Smoothened (Smo).[7] *PTCH* has been identified as an atypical tumour suppressor gene, although only three cases of RMS in NBCCS patients have been documented.[3,5] Nevertheless, the *PTCH* locus (9q22.3) is frequently deleted in embryonal RMS (ERMS).[8] *Ptch* mutations can phenocopy Shh binding, which derepresses Smo signalling and activates its downstream mitogenic effects in mesenchymal precursors. In derived connective tissue, murine models of *Ptch* haploinsufficiency (*Ptch*+/–) spontaneously develop soft tissue sarcomas.[3,6,9]

We have characterised these soft tissue tumours as a model system in order to identify pathways and processes that murine RMS share with human RMS in general. Microarray gene expression profiling and validation studies revealed overexpression of Secreted Phosphoprotein 1 (*Spp1*, also known as Osteopontin, Bone sialoprotein 1 and Early T-lymphocyte activation 1), Matrix Metalloproteinase-2 (*Mmp2*), Matrix Metalloproteinase-14 (*Mmp14*) and nuclear factor-kappa B (NF-κB) subunit p65 (*RelA*) in murine and human tumour samples. Furthermore, plasma samples from RMS patients contain significantly higher levels of SPP1 than controls. Reducing extracellular Spp1 in dissociated *Ptch* +/– mouse RMS cultures with neutralising Spp1 antibody decreased their *Mmp14* RNA expression. Since Spp1 and matrix metalloproteinases (Mmps) can modulate extracellular matrix (ECM) to regulate tumour invasion and metastasis,[10,11] we hypothesise, based on our results, that overexpression of Spp1 and associated Mmp activation constitute a putative signal pathway involved in RMS growth, invasion and metastasis.

2. Materials and methods

2.1. Murine tissue processing and cell culture

Patched haploinsufficient mice (*Ptch*+/– (*Ptch*^{tm1Mps}), Jackson Laboratories, Bar Harbor, ME, United States of America) were maintained on a C57Bl6 background, according to institutional and federal guidelines. Tumours were dissected from normal surrounding tissue and removed from anaesthetised animals, immediately snap-frozen in liquid nitrogen for RNA and protein preparation or divided for cell culture and post-fixation for further histologic processing (see below). Cardiac and skeletal muscle (gastrocnemius) specimens from unaffected age-matched *Ptch*+/– mice were similarly processed. Dissociated cell cultures were prepared from RMS specimens by mincing fresh tumour followed by sequential enzymatic dissociation in collagenase (0.1% w/v, for 10–20 min at 37 °C (Worthington, Lakewood, NJ, USA)) and then Dnase I (200 U/mL, for 5 min at 37 °C (Worthington)). After trituration, single cell suspensions were plated at 2E4 cells per cm^2 on either tissue culture plates (Corning Life Sciences, Lowell, MA, USA) or glass coverslips (Bellco, Vineland, NJ, USA), and in Dulbecco's Modified Eagle's Media (Invitrogen, Carlsbad, CA, USA) supplemented with 20% v/v heat-inactivated foetal calf serum and sodium pyruvate, and maintained at 37 °C in 5% CO_2. The neutralising anti-Spp1 antibody was diluted in complete media before addition to adherent RMS cultures at a final concentration of 1–5 μg/mL (O7635, Sigma Immunochemicals, Saint Louis, MO, USA). After 48 h, cultures were washed and snap-frozen and stored at −80 °C.

2.2. Gene expression microarray analysis

Total cellular RNA was extracted from snap-frozen tumours using TRIzol according to the manufacturer's instructions (Invitrogen). Cardiac muscle from 12 adult *Ptch*+/– mice was pooled to provide a source of reference RNA for microarray and quantitative real-time reverse transcriptase polymerase chain reaction (quantitative real-time RT-PCR) experiments. RNA quantity and integrity were assessed by NanoDrop ND-1000 spectrophotometer (NanoDrop, Wilmington, DE, USA) and Agilent 2100 Bioanalyzer (Agilent Technologies, Santa Clara, CA, USA), respectively. Total cellular RNA from 13 murine RMSs were analysed on commercially available cDNA mouse 15k microarrays (University of Toronto, Toronto, Ontario, Canada; http://www.microarrays.ca/).

Briefly, cDNA was reverse transcribed from 30 μg of each total cellular RNA specimen using Mo-MLV reverse transcriptase (Invitrogen), Oligo(dT) primers and dTTP with amino allyl-labelled dUTP using the Amino Allyl cDNA Labeling Kit according to the manufacturer's instructions (Ambion, Austin, TX, USA). Tumour and control cDNA were labelled with the fluorophores Cy3 (probe) and Cy5 (control), respectively (Amersham Biosciences, Piscataway, NJ, USA). Labelled cDNA were co-hybridised onto microarrays for 18 h at 37 °C in hybridisation buffer (5×SCC, 0.1% SDS w/v, 50% formamide v/v) with mouse Cot-1 DNA (Invitrogen). After successively washing the slides in SDS/SSC buffers with increasing stringency, microarrays were scanned using a Perkin–Elmer 4000XL (Perkin–Elmer, Wellesley, MA, USA) with scan density set at 10 μm for each dye separately. PMT gain and laser power were manually adjusted based on spot intensity (signal saturation) and background. Scanning results were quantitated using Scan Array Express (Perkin–Elmer); immobilised DNA targets were identified by overlaying a grid on the images combined for the two dyes. The raw intensity of each spot was background subtracted and then normalised by the global LOWESS method as implemented in BRB Array Tools, v 3.1.[12] To detect differentially expressed genes, data were analysed with 2-sample t-test with a randomised variance model using BRB Array Tools. Data were also analysed with SAM (Significance of Microarray Analysis) software using log 2 values for a 2-class comparison with unpaired data and

k-Nearest Neighbours imputer.[13,14] Parameters were set to a false discovery rate of less than 1%. Significance of differential expression was calculated as a *q*-value, which is the analogue of the *p*-value for false discovery rate.

2.3. Quantitative real time-reverse transcriptase PCR (quantitative real-time RT-PCR)

First strand cDNA synthesis was performed using Mo-MLV reverse transcriptase (Invitrogen), according to the manufacturer's instructions. PCRs were performed as triplicates in a 20 μL final volume containing template cDNA, SybrGreen Supermix (ABI, Applied Biosystems, Foster City, CA, USA) and specific primers for 40 cycles: 15 s at 95 °C for denaturation, followed by 1 min at 60 °C for annealing/extension. Primer sequences included *Spp1* (+778/+927: forward 5′-TCCCTCGATGTCATCCCTGTTG-3′ and reverse 5′-GGCACTCTCCTGGCTCTCTTTG-3′, yielding a 150 bp target product), *Mmp2* (+2130/+2254: forward 5′-CTGGAATGCCATCCCTGATAA-3′ and reverse 5′-CAAACTTCACGCTCTTGAGACTTT-3′, 125 bp product), *Mmp14* (+1972/+2123: forward 5′-CGTTCGCTGCTGGACAAGG-3′ and reverse 5′-GACTGAGAAGGGAGGCTGGAG-3′, 152 bp product), 18*S* ribosomal RNA (rRNA) (+879/+994: forward 5′-CGGTTCTATTTTGTTGGTTTTCG-3′ and reverse 5′-GCTCTGGTCCGTCTTGCG-3′, 116 bp product). Amplification products were verified by melting curves, agarose gel electrophoresis and sequencing. Results were internally normalised to 18*S* rRNA expression, quantitated relative to *Ptch*+/− murine cardiac and skeletal muscle tissue as tissue controls, and represent the average of at least three independent experiments.

2.4. Immunocytochemistry and Western immunoblot analysis

For immunohistochemical analysis, tissue specimens were post-fixed in 4% paraformaldehyde (PFA, w/v in PBS) and paraffin embedded using standard methods. Fixed deparaffinised tumour sections were processed with primary antibodies listed below, and visualised using standard methods. Briefly, the prepared sections were washed in Tris–EDTA, and endogenous peroxidase was blocked by standard protocols. Biotinylated primary antibody was applied for 25 min at room temperature. Sections were incubated with horseradish peroxidase/streptavidin (BioGenex, San Ramon, CA, USA) for 10 min at room temperature as per standard methods. After counterstaining with hematoxylin, samples were mounted using aqueous mounting medium (Faramount, DAKO, Carpinteria, CA, USA). Positive and negative controls (without primary antibody) were performed with each tissue specimen. No significant staining occurred without primary antibody.

For immunofluorescent analysis of dissociated murine RMS cultures, coverslips were fixed for 10 min in 4% PFA (w/v, PBS), dehydrated in ice-cold 100% methanol and stored at −20 °C. Coverslips were rehydrated and immunostained using standard methods with primary antibodies listed below. Staining with fluorescein isothiocyanate (FITC)-conjugated goat anti-mouse or tetramethyl rhodamine isothiocyanate (TRITC)-conjugated goat anti-rabbit secondary antibodies (Jackson ImmunoResearch Laboratories, West Grove, PA, USA) was detected using a Nikon E600 UV fluorescence microscope.

For Western blotting, snap-frozen tumour samples were lysed in SDS–PAGE-lysis buffer, separated by SDS–PAGE gel electrophoresis, transferred to nitrocellulose membranes (PALL Life Science, East Hills, NY, USA) and immunostained using standard methods and primary antibodies including Spp1 (MPIIIB10, Department of Biology, University of Iowa, Iowa City, IA, USA); NF-κB p65 (sc-372, Santa Cruz Biotechnology, Santa Cruz, CA, USA); activated NF-κB p65, phosphorylated at Serine 536 (S536) (3031S, Cell Signaling, Beverly, MA, USA); Mmp2 (AB809, Chemicon International, Temecula CA, USA); and Mmp14 (IM57, Calbiochem, San Diego, CA, USA); β-actin (sc-8432, Santa Cruz Biotechnology). Binding of fluorescent secondary antibodies, IR800-conjugated goat anti-rabbit (Rockland Immunochemicals, Gilbertsville, PA, USA) and Alexa-Fluor 680-conjugated goat anti-mouse antibodies (Molecular Probes, Eugene, OR, USA), was detected by Li-Cor Odyssey (LI-COR, Lincoln, NE, USA). Immunostaining intensity was quantitated using ImageQuant 5.2 (Molecular Dynamics, Piscataway, NJ, USA). All human tumour and plasma specimens were obtained upon informed consent via institutional review board-approved protocols.

2.5. Enzyme-linked immunosorbent assay (ELISA) analysis

Plasma specimens were obtained from paediatric RMS patients ($n = 17$) upon informed consent to an IRB-approved protocol in accordance with institutional and federal guidelines. RMS histologies included alveolar ($n = 10$) and embryonal ($n = 7$) subtypes and approximately 25% of patients had metastatic disease at presentation. Control plasma samples were obtained from six age-matched non-cancer patients. EDTA-treated whole blood samples were processed using standard methods and stored at −80 °C. Plasma aliquots were assayed with commercially-available Spp1 and total Mmp2 ELISA kits with appropriate negative and positive controls and standards, according to the manufacturer's recommendations (R&D Systems, Minneapolis, MN, USA). Absorbances were quantitated in multiwell plates using a BenchMark Plus plate spectrophotometer (Bio-Rad, Hercules, CA, USA).

3. Results

3.1. Ptch+/− mouse rhabdomyosarcoma characterisation

Mice with heterozygous mutation of *Patched* (*Ptch*+/−) can spontaneously develop soft tissue sarcomas that closely resemble human RMS.[3,6] Approximately, 5% of *Ptch*+/− mice develop RMS as older adults. The onset of RMS is typically detected in adult *Ptch*+/− mice with a median age of 44.3 weeks.

Ptch+/− murine RMS are relatively well defined with focal invasion of adjacent soft tissue, including skeletal muscle (Fig. 1A–B). The tumours were composed of well-differentiated proliferating rhabdomyoblasts of varying size (Fig. 1D, F, H, J). Infrequent elongated spindled rhabdomyoblasts were seen (Fig. 1D). Many of the tumour cells were quite large with eccentric nuclei and abundant deeply eosinophilic cytoplasm, reflecting cytoplasmic myofilaments (Fig. 1H, J).

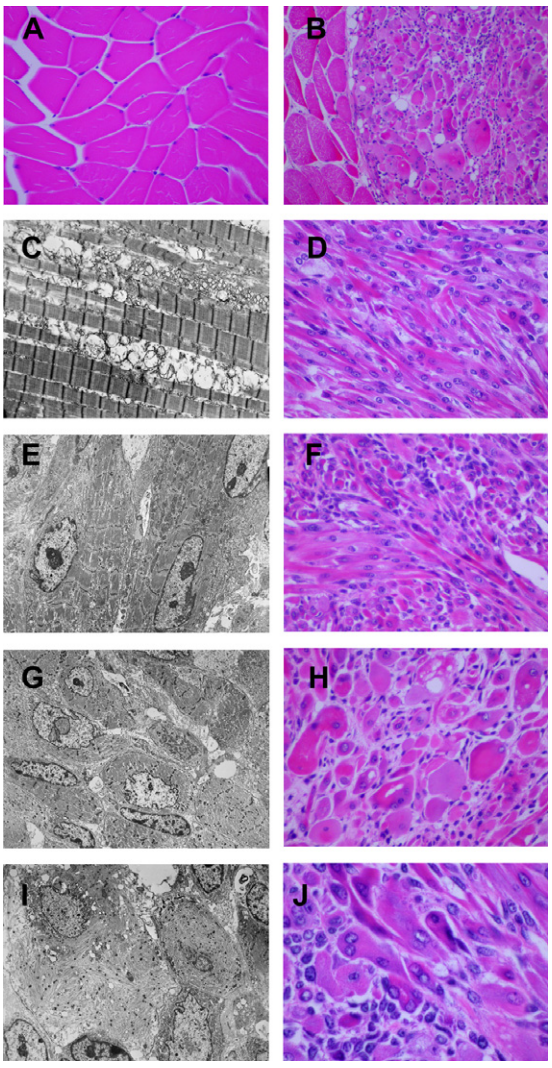

Fig. 1 – *Ptch*+/– mouse soft tissue sarcomas resemble human rhabdomyosarcoma. Hematoxylin/eosin-stained tissue section of (A) skeletal muscle and (B) skeletal muscle and adjacent tumour. (C,E, G, I) Transmission electron microscopy of (C) normal muscle with prominent Z-bands and (E, G, I) rhabdomyosarcoma cells with dysplastic Z-bands. (D, F, H, J) Hematoxylin and eosin-stained tumours sections showing a range of differentiation including, (D) spindle-shaped to (F) intermediate-sized tumour cells and (H, J) larger rhabdomyoblastic cells.

There were also more typical rhabdomyoblasts of intermediate to small size with deeply eosinophilic cytoplasm and a higher nucleus: cytoplasm ratio (Fig. 1F). Transmission electron microscopy demonstrated myofilaments with dysplastic Z-bands (Fig. 1E, G, I) in contrast to the well-organised cytoarchitecture typical of normal mature skeletal muscle (Fig. 1C). Features of human alveolar RMS were not observed.

3.2. *Murine rhabdomyosarcomas overexpress Spp1 RNA*

In order to identify candidate genes in murine RMS for validation in human tumours, we analysed the gene expression profiles of *Ptch*+/– mouse RMS using RNA from 13 tumours with cDNA expression microarrays. Compared to non-tumour control tissue (adult *Ptch*+/– mouse hearts), *Ptch*+/– mouse RMS gene expression profiles reveal differential expression of a wide range of genes associated with tumour growth (select transcripts are shown in Table 1; for a complete list of differentially expressed genes, see Table S1, Supplementary information). Compared to cardiac controls, the IGF signalling-related genes, *Igf2* and *Igfbp5*, were significantly upregulated in RMS, 27.4-fold ±0.14 (mean ± SEM) and 6.8-fold ±0.18-fold, respectively. Another gene involved in muscle differentiation, the *Pax3* downstream target, *Fat tumour suppressor homologue* (*Fath*), was also upregulated (3.1-fold ±0.21). Markers of myogenic differentiation and genes associated with apoptosis were significantly downregulated in RMS compared to controls: *Four-and-a-half LIM domains 2* (*Fhl2*, –9.23-fold ±0.1), *Cysteine rich protein 2* (*Crip2*, –4.3-fold ±0.16), and *Caveolin* (*Cav*, –4.1-fold ±0.17).

Ptch+/– mouse RMS also overexpressed genes encoding adhesion molecules, ECM constituents and angiogenic factors such as pro-collagens, *Lectin* (*Lgals1*) and *Fibronectin* (*Fn1*). In fact, the single most upregulated gene by microarray analysis was *Secreted Phosphoprotein 1* (*Spp1*). Mean *Spp1* RNA levels in *Ptch*+/– mouse RMS were 44.3-fold higher than cardiac control values (±1.3, SEM). *Mmp2* was 1.8-fold higher (±1.2) in RMS compared to controls.

Overexpression of candidate genes implicated by microarray results (*Spp1* and *Mmp2*) was validated in *Ptch*+/– mouse RMS using quantitative real-time RT-PCR. Mean *Spp1* and *Mmp2* RNA expression, internally normalised to 18S rRNA, was 16.3-fold (±0.8, SEM) and 1.8-fold (±0.16) higher than cardiac controls, respectively (Fig. 2A). Although *Mmp14* was not directly implicated by microarray analysis, it has been identified as a downstream transcriptional target of Spp1 signalling; therefore, we assayed its expression by quantitative real-time RT-PCR and found 2.5-fold higher levels (±0.5) than cardiac controls (Fig. 2A). These quantitative real-time RT-PCR results confirmed the overexpression of *Spp1* and *Mmp2* RNA observed by microarray analysis, and implicate *Mmp14* overexpression.

3.3. *Murine rhabdomyosarcoma overexpress Spp1 protein*

To corroborate our microarray and quantitative real-time RT-PCR findings, we assessed protein expression by Western immunoblot analysis. Spp1 is an extensively glycosylated and phosphorylated protein with multiple variant bands. Lysates of *Ptch*+/– mouse RMS reveal that Spp1 isoforms migrate with apparent molecular weights of 20–25, 53–56 and 92 kDa, which are markedly overexpressed by RMS relative to mature striated muscle controls from adult *Ptch*+/– cardiac and gastrocnemius tissues (Fig. 2B–C). On Western blots, Spp1 protein levels in murine RMS were only slightly elevated compared to cardiac controls (3-fold higher ±0.6, mean ± SEM), but this difference was not statistically significant ($P < 0.142$) (Fig. 2B–C). Compared to skeletal muscle, however, RMS displayed 26.7-fold higher levels (±0.10, $P < 0.00002$), indicating a more pronounced expression in heart compared to normal skeletal muscle (Fig. 2B–C).

Ptch+/– mouse RMS display similar total NF-κB p65 protein expression compared to cardiac controls (0.8-fold ±0.26,

Table 1 – Gene expression microarray analysis of *Ptch*+/– mouse rhabdomyosarcoma

Selected differentially expressed murine genes	Symbol	Unigene ID	Fold-difference[a]	*q*-Value
Anthrax Toxin receptor	*Antxr1*	H3075F12	3.7	0.009
TGFβ induced	*Tgfbi*	H3114E06	5.1	0.003
Secreted Phosphoprotein 1 (Osteopontin)	*Spp1*	H3082C12	44.3	0.003
Procollagen	*Col3a1*	H3124H10, H3133G03, H3114H12	7.2	0.003
Fibronectin	*Fn1*	H3116A10	11.5	0.003
Lectin	*Lgals1*	H3009D05, H3003A03	5.1	0.003
Fat tumour suppressor homologue	*Fath*	H3061D06	3.1	0.003
Insulin-like growth factor 2	*Igf2*	H3126A04, H3024B07	27.4	0.003
H19 fetal liver mRNA	*H19*	H3130E06	16.3	0.003
Insulin-like growth factor binding protein 5	*Igfbp5*	H3126F05	6.8	0.003
Four and a half LIM domains 2	*Fhl2*	H3033C07	–4.2	0.003
Cysteine rich protein 2	*Crip2*	H3109H11	–4.2	0.003
Caveolin, caveolae protein	*Cav*	H3089D06	–4.1	0.003

Select genes overexpressed in *Ptch*+/– mouse rhabdomyosarcoma (RMS) samples ($n = 13$), relative to normal mature adult *Ptch*+/– mouse cardiac muscle control tissue.
a (*Fold-change* expressed as mean values relative to reference pooled adult *Ptch*+/– cardiac RNA).

mean ± SEM) (Fig. 2B–C). Westerns blot analysis using a phospho-specific antibody to detect activated p65 revealed a similar pattern of expression in RMS (1.25-fold ±0.6) (Fig. 2B–C). Mean Mmp levels in murine RMS were also markedly elevated. Mmp14 was 4.3-fold higher (±0.9, $P < 0.016$) than cardiac controls, and 10.2-fold higher (±1.38, $P < 0.0066$) than skeletal muscle controls (Fig. 2B–C). Similarly, Mmp2 was 8.67-fold higher (±2.57, $P < 0.0018$) and 4.1-fold higher (±0.79; $P < 0.020$) than cardiac and skeletal muscle controls, respectively (Fig. 2B–C). These immunoblot results corroborate our RNA quantitation demonstrating higher levels of Spp1, Mmp14 and Mmp2 protein expression in *Ptch*+/– mouse RMS compared to mature striated muscle.

Immunohistochemical staining of *Ptch*+/– mouse RMS sections reveals that tumour cells express Spp1 diffusely throughout their cytoplasm (Fig. 2D) compared to normal skeletal muscle, where Spp1 is restricted to ECM and plasma membrane (Fig. 2E). The NF-κB p65 subunit is also diffusely overexpressed in RMS cells with predominantly cytoplasmic localisation, whereas normal muscle lacks significant immunostaining (Fig. 2F–G). Mmp2 is also diffusely and intensely stained in RMS cells, in contrast to muscle (Fig. 2H–I). These immunostaining results validate our Western blot analysis and indicate that *Ptch*+/– mouse RMS diffusely express the constituents of a putative Spp1/NF-κB-mediated signalling pathway known to induce Mmp expression.[10,11]

3.4. *Neutralising Spp1 antibody decreases Mmp14 in murine rhabdomyosarcoma in vitro*

When grown as dissociated short-term cultures, *Ptch*+/– mouse RMS cells adhere avidly and survive in typical cell culture media. Immunofluorescent staining of murine RMS cells cultivated *in vitro* reveals diffuse cytoplasmic expression of β-actin (Fig. 3A). Immunofluorescent staining of Spp1 was more intense in aggregates compared to single dissociated RMS cells (Fig. 3B). RMS cells also display widely distributed NF-κB p65 immunostaining (Fig. 3C), in contrast to membrane-associated expression of Mmp2, especially around clumped cells (Fig. 3D).

To investigate the role of Spp1, we treated *Ptch*+/– mouse RMS cultures with Spp1 antibody previously described with neutralising activity in 293 cells.[15] Because limited cell yields precluded protein analysis, we assayed the resulting changes in RNA expression with quantitative real-time RT-PCR. After 48 h of Spp1 antibody exposure (1 μg/mL), we detected significantly less *Mmp14* RNA (0.5-fold ±0.14, mean ± SEM), compared to control RMS cultures (Fig. 3E). In contrast, *Spp1* RNA expression increased by 1.25-fold (±0.22) after Spp1 antibody treatment. Similar results were observed at higher antibody concentrations (up to 5 μg/mL), which reduced *Mmp14* to 0.3-fold (±0.02) and increased *Spp1* to 1.98-fold (±0.12) compared to controls. In addition to providing evidence for positive regulation of *Mmp14* expression by extracellular Spp1, these antibody-blocking results suggest that Spp1 may also participate in negative feedback regulation of its own transcription.

3.5. *Primary human rhabdomyosarcoma samples overexpress SPP1, NF-κB p65 and MMPs*

Based on our murine results, we evaluated six primary human RMS specimens with Western immunoblots (clinical data are summarised in Table S2, Supplementary information). Compared to normal mature skeletal muscle, human RMS revealed significantly elevated protein expression of candidate genes. SPP1 was overexpressed in tumours as three major isoforms (75–78, 51, and 20 kDa) at mean levels approximately 37-fold (±15.4, ±SEM) relative to mature muscle controls (Fig. 4A–B). Human RMS overexpressed NF-κB p65, 35-fold (±8) and the activated isoform, phosho-p65 (Ser536), 51-fold (±16.1), compared to controls. MMP14 was upregulated 56-fold (±31.5) as 60 and 44–47 kDa bands, corresponding to inactive and cleaved isoforms, respectively. MMP2 was overexpressed 37-fold (±16.3) as 73–77 kDa pro-MMP2 and 61–64 kDa cleaved isoform. These data indicate a wide range of expressions, but markedly higher levels of SPP1, p65, MMP14 and MMP2 in human RMS, raising the possibility that the secreted extracellular factors represent circulating tumour biomarkers.

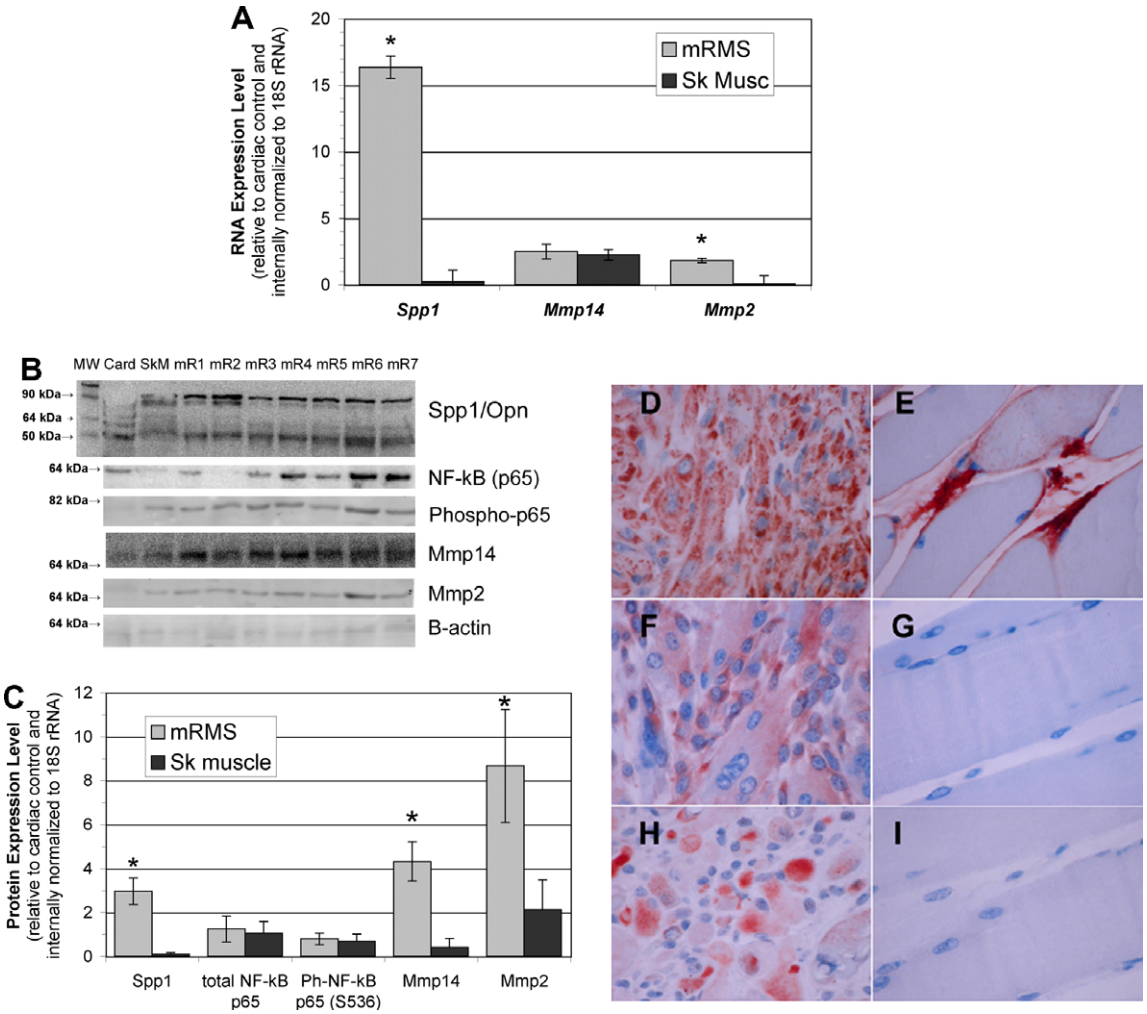

Fig. 2 – *Ptch*+/– mouse rhabdomyosarcoma overexpress *Spp1*, *Mmp14* and *Mmp2*. (A) Quantitative real-time RT-PCR analysis reveals significantly higher mean levels of *Spp1*, *Mmp14* and *Mmp2* RNA in tumour cells relative to normal cardiac reference tissue and internally normalised to 18S rRNA content (error bars, SEM). (B) Western immunoblot analysis of rhabdomyosarcoma and control tissue lysates reveals differential expression of Spp1, total NF-κB p65, Mmp14, and Mmp2 in mature adult *Ptch*+/– mouse cardiac and skeletal muscle tissue controls. (C) Protein expression values for Spp1, total NF-κB p65, phosphorylated NF-κB p65 (Ser536), Mmp14 and Mmp2; relative to cardiac reference tissue and internally normalised to β-actin levels (mean values of at least three experiments; error bars, SEM). (*Statistically significant differences between tumour and normal muscle tissue.) (D–I) Immunostaining of tissue sections from (D, F, H) *Ptch*+/– mouse rhabdomyosarcoma and (E, G, I) normal skeletal muscle reveals tumour overexpression of Spp1 (D, E), NF-κB p65 (F, G) and Mmp2 (H, I). Peroxidase-based immunostaining and hematoxylin counterstaining are detailed in the text.

3.6. *The plasma of rhabdomyosarcoma patients contains elevated levels of circulating Spp1*

Since increased SPP1 and MMP2 have been reported in the plasma of adult solid tumour patients,[16,17] we evaluated their levels in plasma specimens from paediatric RMS patients using ELISA methods (clinical data are summarised in Table S2, Supplemental information). Total MMP2 protein levels in the plasma of RMS patients (245 ng/mL ±18, mean ± SEM; $n = 17$) were not significantly different from controls (373 ng/mL ±37; $n = 6$). SPP1 protein, however, was significantly elevated in plasma from RMS patients (295 ng/mL ±28) compared to normal age-matched controls (78 ng/mL ±12), which agree with reported adult norms ranging from 117 to 155 ng/mL (Fig. 4C).[18]

SPP1 levels did not correlate significantly with either histology (alveolar versus embryonal), the presence of metastases at diagnosis, or other clinical features. These data suggest that circulating SPP1 levels are elevated above the normal range in RMS patients regardless of tumour subtype or spread.

4. Discussion

We have characterised spontaneous soft tissue sarcomas from *Ptch*+/– mice as a model for gene discovery studies of

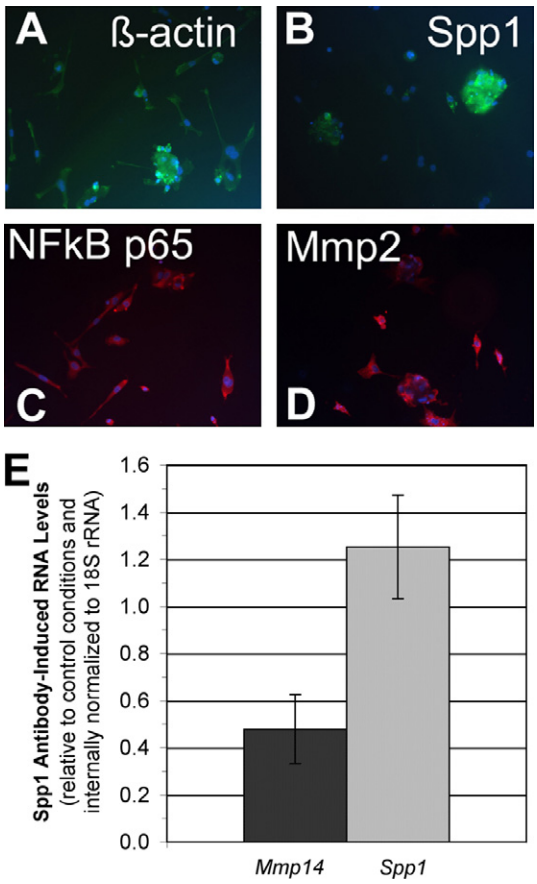

Fig. 3 – *Ptch*+/– mouse rhabdomyosarcoma cell cultures express *Spp1*, NF-κB p65 and *Mmp2*. (A–D) Immunofluorescent staining of *Ptch*+/– mouse rhabdomyosarcoma cultivated *in vitro* reveals (A) diffuse expression of β-actin, (B) Spp1 predominantly detected in clumped cells (both with FITC-conjugated secondary antibodies), whereas (C) NF-κB p65 was widely distributed, and (D) Mmp2 was particularly detected at the edges of clumped cells (both using TRITC-conjugated secondary antibodies). (E) Anti-Spp1 antibody treatment of *Ptch*+/– mouse rhabdomyosarcoma decreases *Mmp14* expression. RNA levels are calculated relative to parallel short term culture under control conditions (error bars, SEM).

human RMS. Based on its appearance morphologically and by electron microscopy, we conclude that the *Ptch*+/– mouse sarcomas represent a developmental neoplasm that displays a range of differentiation similar to the rhabdomyoblastic variant of human RMS. Given the absence of alveolar characteristics, we sought pathways independent of the translocations common to alveolar rhabdomyosarcoma (ARMS). We therefore employed a gene discovery approach to the genomic analysis of this RMS model to identify candidate genes that influence its biological behaviour. Our gene expression analysis of *Ptch*+/– mouse RMS revealed that genes encoding for extracellular matrix proteins are highly overexpressed in tumours compared to mature striated muscle, especially *Spp1*. *Spp1* overexpression in *Ptch*+/– mouse RMS is not surprising since it is a transcriptional target of Gli (*Gli1*) induced by *Ptch* haploinsufficiency and Shh signalling (Fig. 5).[19] We selected adult cardiac muscle as the reference tissue control for our microarray analysis of RMS gene expression to identify markers that potentially distinguish neoplastic from terminally differentiated muscle cells.

Other investigators have pursued similar gene discovery approaches but employed different reference tissues. Several studies have used a microarray profiling approach to identify differentially expressed genes in mouse and human RMS. Kappler and colleagues analysed sarcomas from a different *Ptch* heterozygous mouse model using a custom human cDNA microarray to identify 31 out of 430 clones that were differentially expressed compared to a universal reference RNA pool, representing multiple cell types.[20] They did not detect differential expression of ECM proteins, although we confirmed tumour overexpression of *Igf2* and related genes that they documented.[3,20] However, their subsequent analysis of *Ptch* and derived compound *Trp53* heterozygous mouse sarcomas reveals differential expression of ECM proteins, including procollagens and Mmp9.[21] Unfortunately, because of differences in mouse strains, platform and controls, our results are not directly comparable.

Several gene expression profiling studies of human RMS support the possible involvement of tumour microenvironment in tumour growth, as indicated by the dysregulation of genes encoding for ECM proteins. Khan and colleagues[22,23] used a cDNA platform to demonstrate that the presence of t(2;13) induces a specific transcription program, distinct from other tumours. Their subsequent analysis yielded a 96 gene predictor that could accurately classify several types of small round blue cell tumours. For example, RMS displayed higher levels of ECM genes such as collagens.[24] Wachtel and colleagues determined characteristic expression profiles among ERMS, translocation-positive and -negative ARMS. Among their oligonucleotide microarray-based RMS 'signatures', *ADAM10* was the only gene encoding an ECM protein.[25] Baer and colleagues compared the gene expression profiles of RMS and Ewing's sarcoma, and detected the up-regulation in RMS of several ECM genes, particularly collagens and integrin-7.[26] De Pittà and colleagues employed dedicated muscle cDNA microarrays, but detected downregulation of ECM constituents (laminin and lectin) in ARMS compared to foetal skeletal muscle.[27] Davicioni and colleagues recently reported that several genes encoding ECM constituents are upregulated in *PAX3/7-FKHR* translocation-positive RMS and cell lines including collagens, MMPs and laminin. However, *MMP2* was downregulated.[28] Romualdi and colleagues conducted a meta-analysis of five different microarray profile studies of RMS. Among 153 commonly differentially regulated genes, the laminin receptor was the only ECM gene included in the list.[29] Since each microarray analysis examined different tumours, utilised different platforms, references and analytical approaches, direct comparison of their results remains a challenge.

Regardless of the choice of platform or controls, formulation of hypotheses based on gene discovery approaches and expression microarray analyses requires stringent validation of candidates. Indeed, we have confirmed elevated Spp1/SPP1 expression at the protein level in both murine and human RMS, compared to adult differentiated muscle. Because inhibition of Spp1 decreases the growth of transformed mur-

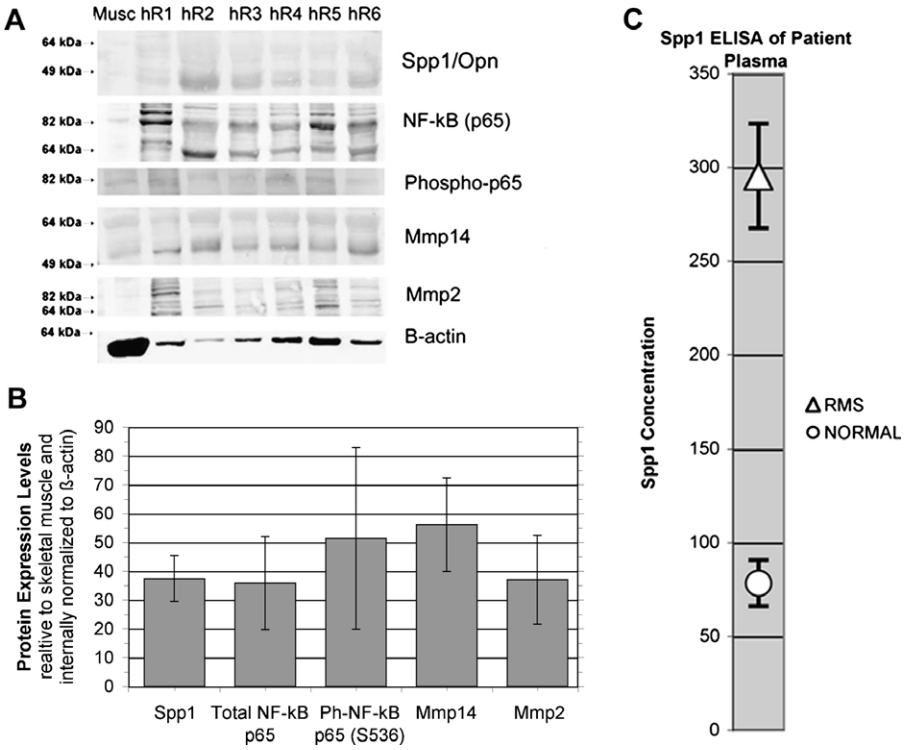

Fig. 4 – Human rhabdomyosarcomas overexpress Spp1, NF- κB p65, MMP14 and MMP2. (A) Western blots of primary human rhabdomyosarcoma specimens for Spp1, total NF-κB p65, phosphorylated NF-κB p65 (Ser536), Mmp14 and Mmp2 (B) Mean protein expression of Spp1, total NF-κB p65, phosphorylated NF-κB p65 (Ser536), Mmp14, and Mmp2 in primary human rhabdomyosarcoma specimens, relative to mature skeletal muscle and internally normalised to β-actin levels (error bars: SEM). (C) ELISA analysis reveals significantly higher Spp1 levels in plasma from rhabdomyosarcoma patients ($n = 17$) compared to samples from age-matched controls ($n = 6$) (error bars, SEM).

ine fibroblasts, we sought to test the effects of blocking Spp1 in *Ptch+/–* mouse RMS cultures using a neutralising antibody.[15] The decreased *Mmp14* expression observed in response to Spp1-blocking antibody is consistent with earlier reports that Spp1 induces *Mmp14* expression, which in turn activates Mmp2.[10] Spp1 reportedly stimulates growth and NF-κB-mediated induction of *Mmp14*, *Mmp9*, and activation of Mmp2 in murine melanoma cells.[10,11] NF-κB is a transcription complex that consists of a dimer of subunits encoded by *Nfkb1* or *Nfkb2*; bound to *RelA* (p65), *Rel*, or *Relb*. NF-κB regulates growth factor expression, stress and immune responses, adhesion, inflammation and apoptosis.[30] This cascade represents a signalling pathway implicated in local tissue invasion by tumour cells.

SPP1 is an extensively phosphorylated and glycosylated secreted protein found in normal connective tissue that binds transmembrane $\alpha v\beta_3$ integrin receptors (Fig. 5).[31] Spp1 is developmentally upregulated during myogenesis and muscle differentiation.[32] The importance of ECM and other microenvironmental factors in the regulation of RMS growth has been suggested by surveys of human tumour specimens. SPP1 and constituents of ECM can regulate tumour growth as well as muscle differentiation.[33,34] *SPP1* is also a transcriptional target of p53 and is widely expressed in adenocarcinomas and squamous cell carcinomas, and upregulated in breast and ovarian cancers.[15,35–37] SPP1 has been identified as a biomarker associated with worse outcome and increased histologic grade.[37] For example, SPP1 expression by breast and several other tumours appeared to increase invasion.[35,38] Inhibition of Spp1 reduced the growth of experimentally transformed fibroblasts.[15] Spp1 has also been implicated in tumour-associated angiogenesis by its induction of migration and its cooperative effects with vascular endothelial growth factor.[39]

Candidate mechanisms responsible for the biological effects associated with SPP1 include its induction and activation of downstream matrix metalloproteinases (MMPs) (Fig. 5). SPP1 and MMPs have been actively studied as key regulators of tumour microenvironment.[40] MMPs are Zn^{2+}-binding endopeptidases (encoded by different genes) that degrade various ECM components with different substrate specificities. MMPs are overexpressed by a variety of cancer types and are implicated in tissue remodelling, local invasion, migration, angiogenesis, and metastatic spread.[40] Tissue inhibitors of metalloproteinases (TIMPs) are a family of low-molecular weight proteins that modulate MMP activity depending on its membrane-associated concentration.[40]

MMP14 is a widely expressed protein with a transmembrane domain anchoring it to the cell surface that distinguishes it from other MMPs. MMP14 in conjunction with TIMP2 cleaves extracellular pro-MMP2 in addition to degrading collagens in ECM. *MMP2* encodes pro-MMP2, an inactive secreted pro-enzyme that requires extracellular proteolytic cleavage for activation.[40] When activated by MMP14

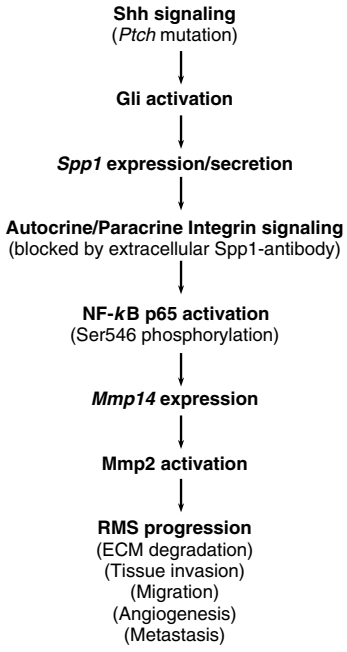

Fig. 5 – Proposed Model for Spp1-induced Mmp Activation in rhabdomyosarcoma. For details and references, refer to text. Briefly, *Spp1* is a transcriptional target of Gli induced by *Ptch* haploinsufficiency in *Ptch*+/– mouse RMS. Spp1 binds transmembrane integrin receptors, inducing and activating downstream Mmps via NF-kB transcriptional activity. Spp1 and Mmps are key regulators of tumor–microenvironment interactions. Spp1 signalling may act in a autocrine-paracrine manner via NF-kB to induce downstream Mmp activation to increase rhabdomyosarcoma invasiveness.

(Mt1-Mmp), MMP2 (gelatinase A (72 kDa)) cleaves type IV collagen, a major structural component of basement membranes. Activated MMP2 has also been linked to the invasive potential and pro-angiogenic properties of malignant cells.[41] Diomedi-Camassei and colleagues detected increased levels of MMP-1, -2, -9 in human RMS of alveolar histology, compared to low or negative immunostaining in less aggressive ERMS.[42] Onisto and colleagues detected increasing MMP2 activity that correlated with a potentiated *in vitro* invasion of an RMS cell line after transfection with a *PAX3-FKHR* construct.[43]

Because of the potential clinical significance of Spp1/ NF-κB/Mmp2 activation, we assayed levels of SPP1 and MMP2 in RMS patient plasma samples obtained at the time of diagnosis. The elevated levels of SPP1 in RMS patients, compared to age-matched normal controls, suggest that human RMS-secreted SPP1 represents a circulating biomarker. Since several studies reported that higher plasma SPP1 levels in patients with different kinds of cancers may be associated with decreased survival, our findings support future correlative studies of the potential clinical significance of SPP1 in diagnosis and prognosis of RMS.[17,18]

In conclusion, we hypothesise that Spp1 signalling acts in an autocrine–paracrine manner via NF-κB to induce downstream Mmp activation, which increases RMS invasiveness. Our characterisation of the *Ptch*+/– murine model of RMS provides evidence for the induction of downstream Mmp synthesis and activation as one of the biological effects of Spp1 overexpression. These murine data and our analysis of plasma from paediatric patients support our hypothesis that expression of *SPP1* upregulates the expression and activation of MMPs in RMS.

Conflict of interest statement

None declared.

Acknowledgements

We thank Linda L. Lin, Diana Joo Youn Hwang, Sowmya Paturi, Jessen A. Rajan, Cindy C. Rho, Charlotte R. Nicholson and Dorene M. Rudman for their technical assistance; Laszlo Perlaky for assistance with tissue procurement and Angelo Rosolen and Lee Helman for helpful discussions.

Funding sources. This work was supported by Associazione Italiana contro le Leucemie (M.D.B.); the John S. Dunn Research Foundation; the Pediatric Brain Tumor Foundation of the United States (J.M.S.); Hope Street Kids (J.Y.H.K.); NIH Grants HD042977 (R.C.C.), HD041648 and NS043517 (J.Y.H.K.); and John and Carroll Goodman (J.Y.H.K.).

Appendix A. Supplementary data

Supplementary data associated with this article can be found, in the online version, at doi:10.1016/j.ejca.2007.02.008.

REFERENCES

1. Anderson J, Gordon A, Pritchard-Jones K, Shipley J. Genes, chromosomes, and rhabdomyosarcoma. *Gene Chromosome Cancer* 1999;**26**(4):275–85.
2. McDowell HP. Update on childhood rhabdomyosarcoma. *Arch Dis Child* 2003;**88**(4):354–7.
3. Hahn H, Wojnowski L, Specht K, et al. Patched target Igf2 is indispensable for the formation of medulloblastoma and rhabdomyosarcoma. *J Biol Chem* 2000;**275**(37):28341–4.
4. Li FP, Fraumeni Jr JF. Rhabdomyosarcoma in children: epidemiologic study and identification of a familial cancer syndrome. *J Natl Cancer Inst* 1969;**43**(6):1365–73.
5. Gorlin RJ. Nevoid basal cell carcinoma syndrome. *Dermatol Clin* 1995;**13**(1):113–25.
6. Goodrich LV, Milenkovic L, Higgins KM, Scott MP. Altered neural cell fates and medulloblastoma in mouse patched mutants. *Science* 1997;**277**(5329):1109–13.
7. Toftgard R. Hedgehog signalling in cancer. *Cell Mol Life Sci* 2000;**57**(12):1720–31.
8. Bridge JA, Liu J, Weibolt V, et al. Novel genomic imbalances in embryonal rhabdomyosarcoma revealed by comparative genomic hybridization and fluorescence in situ hybridization: an Intergroup Rhabdomyosarcoma Study. *Gene Chromosome Cancer* 2000;**27**(4):337–44.
9. Pazzaglia S. Ptc1 heterozygous knockout mice as a model of multi-organ tumorigenesis. *Cancer Lett* 2006;**234**(2):124–34.
10. Philip S, Bulbule A, Kundu GC. Osteopontin stimulates tumor growth and activation of promatrix metalloproteinase-2

through nuclear factor-kappa B-mediated induction of membrane type 1 matrix metalloproteinase in murine melanoma cells. *J Biol Chem* 2001;**276**(48):44926–35.
11. Rangaswami H, Bulbule A, Kundu GC. Nuclear factor-inducing kinase plays a crucial role in osteopontin-induced MAPK/IkappaBalpha kinase-dependent nuclear factor kappaB-mediated promatrix metalloproteinase-9 activation. *J Biol Chem* 2004;**279**(37):38921–35.
12. BRB Array Tools v3.1. Integrated package for the visualization and statistical analysis of DNA microarray gene expression data. <http://linus.nci.nih.gov/BRBArrayTools.html> [computer program]. National Cancer Institute and the Emmes Corporation; 1999.
13. Tusher VG, Tibshirani R, Chu G. Significance analysis of microarrays applied to the ionizing radiation response. *Proc Natl Acad Sci USA* 2001;**98**(9):5116–21.
14. SAM: Significant Analysis of microarrays; supervised learning software for genomic expression data mining. <http://www-stat.stanford.edu/~tibs/SAM/> [computer program]. Stanford University Lab; 2005.
15. Behrend EI, Craig AM, Wilson SM, et al. Reduced malignancy of ras-transformed NIH 3T3 cells expressing antisense osteopontin RNA. *Cancer Res* 1994;**54**(3):832–7.
16. Schorge JO, Drake RD, Lee H, et al. Osteopontin as an adjunct to CA125 in detecting recurrent ovarian cancer. *Clin Cancer Res* 2004;**10**(10):3474–8.
17. Overgaard J, Eriksen JG, Nordsmark M, et al. Plasma osteopontin, hypoxia, and response to the hypoxia sensitiser nimorazole in radiotherapy of head and neck cancer: results from the DAHANCA 5 randomised double-blind placebo-controlled trial. *Lancet Oncol* 2005;**6**(10):757–64.
18. Singhal H, Bautista DS, Tonkin KS, et al. Elevated plasma osteopontin in metastatic breast cancer associated with increased tumor burden and decreased survival. *Clin Cancer Res* 1997;**3**(4):605–11.
19. Yoon JW, Kita Y, Frank DJ, et al. Gene expression profiling leads to identification of GLI1-binding elements in target genes and a role for multiple downstream pathways in GLI1-induced cell transformation. *J Biol Chem* 2002;**277**(7):5548–55.
20. Kappler R, Calzada-Wack J, Schnitzbauer U, et al. Molecular characterization of Patched-associated rhabdomyosarcoma. *J Pathol* 2003;**200**(3):348–56.
21. Kappler R, Bauer R, Calzada-Wack J, Rosemann M, Hammerlein B, Hahn H. Profiling the molecular difference between Patched- and p53-dependent rhabdomyosarcoma. *Oncogene* 2004;**23**(54):8785–95.
22. Khan J, Simon R, Bittner M, et al. Gene expression profiling of alveolar rhabdomyosarcoma with cDNA microarrays. *Cancer Res* 1998;**58**(22):5009–13.
23. Khan J, Bittner ML, Saal LH, et al. cDNA microarrays detect activation of a myogenic transcription program by the PAX3-FKHR fusion oncogene. *Proc Natl Acad Sci USA* 1999;**96**(23):13264–9.
24. Khan J, Wei JS, Ringner M, et al. Classification and diagnostic prediction of cancers using gene expression profiling and artificial neural networks. *Nat Med* 2001;**7**(6):673–9.
25. Wachtel M, Dettling M, Koscielniak E, et al. Gene expression signatures identify rhabdomyosarcoma subtypes and detect a novel t(2;2)(q35;p23) translocation fusing PAX3 to NCOA1. *Cancer Res* 2004;**64**(16):5539–45.
26. Baer C, Nees M, Breit S, et al. Profiling and functional annotation of mRNA gene expression in pediatric rhabdomyosarcoma and Ewing's sarcoma. *Int J Cancer* 2004;**110**(5):687–94.
27. De Pittà C, Tombolan L, Albiero G, et al. Gene expression profiling identifies potential relevant genes in alveolar rhabdomyosarcoma pathogenesis and discriminates PAX3-FKHR positive and negative tumors. *Int J Cancer* 2006;**118**(11):2772–81.
28. Davicioni E, Finckenstein FG, Shahbazian V, Buckley JD, Triche MJ, Anderson MJ. Identification of a PAX-FKHR gene expression signature that defines molecular classes and determines the prognosis of alveolar rhabdomyosarcomas. *Cancer Res* 2006;**66**(14):6936–46.
29. Romualdi C, De Pittà C, Tombolan L, et al. Defining the gene expression signature of rhabdomyosarcoma by meta-analysis. *BMC Genomics* 2006;**7**:287.
30. Panwalkar A, Verstovsek S, Giles F. Nuclear factor-kappaB modulation as a therapeutic approach in hematologic malignancies. *Cancer* 2004;**100**(8):1578–89.
31. Hu DD, Lin EC, Kovach NL, Hoyer JR, Smith JW. A biochemical characterization of the binding of osteopontin to integrins alpha v beta 1 and alpha v beta 5. *J Biol Chem* 1995;**270**(44):26232–8.
32. Pereira RO, Carvalho SN, Stumbo AC, et al. Osteopontin expression in coculture of differentiating rat fetal skeletal fibroblasts and myoblasts. *In Vitro Cell Dev Biol Anim* 2006; **42**(1–2):4–7.
33. Osses N, Brandan E. ECM is required for skeletal muscle differentiation independently of muscle regulatory factor expression. *Am J Physiol Cell Physiol* 2002;**282**(2):C383–94.
34. Stracca-Pansa V, Dickman PS, Zamboni G, Bevilacqua PA, Ninfo V. Extracellular matrix of small round cell tumors of childhood: an immunohistochemical study of 67 cases. *Pediatr Pathol* 1994;**14**(1):111–25.
35. Kim JH, Skates SJ, Uede T, et al. Osteopontin as a potential diagnostic biomarker for ovarian cancer. *JAMA* 2002;**287**(13):1671–9.
36. Furger KA, Menon RK, Tuck AB, Bramwell VH, Chambers AF. The functional and clinical roles of osteopontin in cancer and metastasis. *Curr Mol Med* 2001;**1**(5):621–32.
37. Coppola D, Szabo M, Boulware D, et al. Correlation of osteopontin protein expression and pathological stage across a wide variety of tumor histologies. *Clin Cancer Res* 2004;**10**(1 Pt 1):184–90.
38. Furger KA, Allan AL, Wilson SM, et al. Beta(3) integrin expression increases breast carcinoma cell responsiveness to the malignancy-enhancing effects of osteopontin. *Mol Cancer Res* 2003;**1**(11):810–9.
39. Hirama M, Takahashi F, Takahashi K, et al. Osteopontin overproduced by tumor cells acts as a potent angiogenic factor contributing to tumor growth. *Cancer Lett* 2003;**198**(1):107–17.
40. Curran S, Murray GI. Matrix metalloproteinases: molecular aspects of their roles in tumour invasion and metastasis. *Eur J Cancer* 2000;**36**(13 Spec. No.):1621–30.
41. Klein G, Vellenga E, Fraaije MW, Kamps WA, de-Bont ES. The possible role of matrix metalloproteinase (MMP)-2 and MMP-9 in cancer, e.g. acute leukemia. *Crit Rev Oncol Hematol* 2004;**50**(2):87–100.
42. Diomedi-Camassei F, Boldrini R, Rava L, et al. Different pattern of matrix metalloproteinases expression in alveolar versus embryonal rhabdomyosarcoma. *J Pediatr Surg* 2004;**39**(11):1673–9.
43. Onisto M, Slongo ML, Gregnanin L, et al. Expression and activity of vascular endothelial growth factor and metalloproteinases in alveolar and embryonal rhabdomyosarcoma cell lines. *Int J Oncol* 2005;**27**(3):791–8.